Microradiography as a Tool to Detect Heavy Metal Uptake in Plants for Phytoremediation Applications

LUCIA REALE,[1]* ANTONIA LAI,[2] IDA BELLUCCI,[3] ANATOLY FAENOV,[4] TATIANA PIKUZ,[4] FRANCESCO FLORA,[2] LAURA SPANÒ,[5] ANNA POMA,[5] TANIA LIMONGI,[1] LIBERO PALLADINO,[1] ANTONIO RITUCCI,[1] GIUSEPPE TOMASSETTI,[1] GIOVANNI PETROCELLI,[3] AND SERGIO MARTELLUCCI[3]
[1]*Università di L'Aquila, Dipartimento di Fisica and INFM, INFN-LNGS- L'Aquila, Italy*
[2]*ENEA, Unità Tecnico Scientifica di Fisica Applicata, 00044 Frascati, Italy*
[3]*Università di Roma Tor Vergata, Dipartimento STFE (scienze e tecnologie fisiche ed energetiche)-INFM unità di ricerca di Tor Vergata, Rome, Italy*
[4]*Multicharged Ions Spectra Data Center of VNIIFRTI, Mendeleevo, Moscow Region, 141570, Russia*
[5]*Università di L'Aquila, Dipartimento di Biologia di Base ed Applicata, Coppito L'Aquila, Italy*

KEY WORDS microradiography; plant leaves; phytoremediation; X-rays

ABSTRACT In this paper, an application of contact microradiography with soft X-rays for detecting the uptake site of heavy metal in the whole plant leaves is investigated. The X-ray source is a laser-plasma one based on an Nd:glass laser. The soft X-ray radiation emitted from the plasma laser targets of magnesium, iron, and copper can be strongly absorbed in the leaves' regions rich in iron, magnesium, and copper. This absorbance could point to structures in the leaves where these heavy elements are found. In this work, leaves treated with copper sulfate diluted in water at 1, 2, and 5% were imaged by using a copper target, in order to evaluate differences with untreated control leaves. Our results showed that this methodology highlighted the presence of copper in the treated leaves. This new methodology should detect heavy element pollutants inside plants and it should also be a useful analytic tool in phytoremediation studies. *Microsc. Res. Tech. 69:666–674, 2006.*

INTRODUCTION

Traditional techniques for biological imaging are well known: light microscopy (LM), utilized for over 300 y, and electron microscopy (transmission electron microscopy (TEM) and SEM) introduced in the1950s. These techniques are limited, which has stimulated research into other types of microscopic imaging. Normal LM has a resolution limit of about 250 nm, governed by the wavelength of visible light and specimen-staining techniques, which often modify the normal living state morphology; whereas, TEM, with short wavelengths of accelerated electrons, can give a resolution of 1–2 Å. Biological sample preparation generally requires specimen dehydration, fixing, and staining with electron-dense substances such as osmium tetraoxide and lead salts, which make it impossible to look at the preserved living state but with greatly enhanced electron scattering and contrast.

A different technique for TEM, which reduces some of the above-mentioned problems, is the negative staining technique which uses heavy metals that form a glass-like matrix around the biological materials. This technique is quite useful for imaging parts of cells or macromolecules, but the samples are dehydrated and surrounded by a stain matrix.

To minimize the problem of sample preparation artifacts, imaging the internal structure of living cells in their normal living state by means of an X-ray microscope has been pursued by biologists and physicists for many years. (Cotton et al., 1992, 1995; Fletcher et al., 1992; Ford et al., 1991; Panessa et al., 1981; Panessa-Warren et al., 1989, 1991; Stead et al., 1988, 1992).

This aim has created the soft-X-ray microscopy (i.e., the observation of individual cells or a few cells under low energy X-rays) and microradiography (i.e., the observation of small insects or plants generally imaged on a high-resolution photographic film), which were introduced for imaging the internal structure of cells and small biological samples in their normal living state. In fact, imaging with soft X-rays offers the possibility of viewing the internal structure of totally intact living biological specimen at a resolution slightly better than that of LM, while avoiding the dehydration and staining of specimens for TEM.

Soft-X-ray microscopy is of particular interest in the region of the X-ray spectrum between 2.3 and 4.4 nm (0.28–0.53 keV), known as the "water-window." This region lies between the oxygen and the carbon k-absorption edges (Fig. 1). In this region, the absorption of carbon is ~10 times that of water. Hence, using X-rays in this range allows living biological specimens to be imaged with good contrast in a natural aqueous environment (Stead et al., 1988, 1992; Albertano et al., 1997a).

During the last 10 y, soft-X-rays produced by laser plasmas have been widely used for the imaging tech-

*Correspondence to: Lucia Reale, c/o Prof. Giuseppe Tomassetti, Università di L'Aquila, Dipartimento di Fisica and INFM, INFN-LNGS Via Vetoio, Coppito 67010 L'Aquila, Italy. E-mail: lucia.reale@gmail.com

Abbreviations: AFM, atomic force microscope; LM, light microscopy; PMMA, poly-methyl-methacrylate; SEM, scanning electron microscope; SXCM, soft X-ray contact microscopy; TEM, transmission electron microscope

Received 8 September 2005; accepted 16 March 2006

DOI 10.1002/jemt.20350

Published online 20 June 2006 in Wiley InterScience (www.interscience.wiley.com).

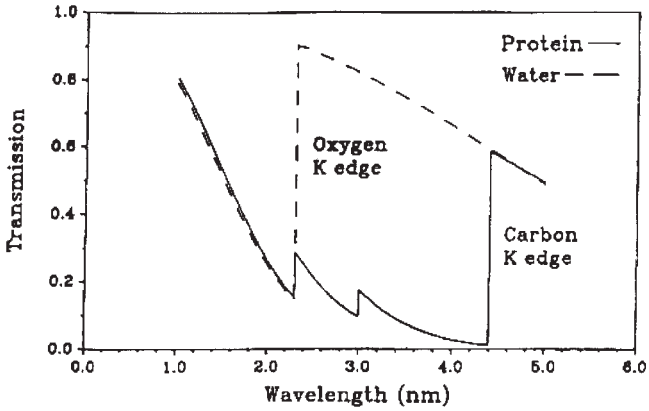

Fig. 1. Transmission in the water-window spectral region of water and carbon, 1 μm in thickness (Cotton et al., 1993).

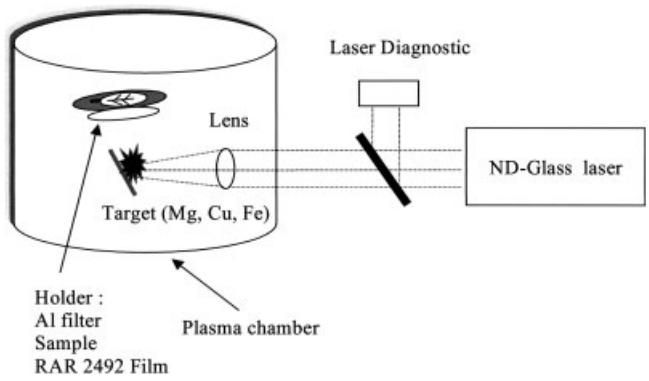

Fig. 2. Experimental layout for X-ray contact microradiography by laser-generated plasma.

nique called the "contact mode" (SXCM), which places the sample in contact with a photosensitive plate, typically a PMMA (poly methyl methacrylate) photoresist for standard radiography (Albertano et al., 1997a, 1997b; Bollanti et al., 1995, 1996, 1998; Conti et al., 1997; Cotton et al., 1995; Fletcher et al., 1992; Ford et al., 1991; Stead et al., 1988).

Alternatively, monochromatic X-ray sources from a synchrotron source with a Fresnel zone plate lenses to project the magnified image on a CCD have been employed (Medenwaldt et al., 1998).

In the SXCM, the photoresist PMMA, after the development, assumes a relief map of the cell image, which can be analyzed with AFM, giving a final resolution of 50–100 nm, limited mainly by diffraction effects and by lateral erosion of the PMMA during its development. Instead, in contact microradiography, the specimen resolution is generally limited by the dimensions of the emulsion grains in the film to a few microns.

As mentioned earlier, there is also an alternative procedure to both techniques, using optical elements which magnify (i.e., a zone plate lens or a Schwarzschild multilayer mirrors couple for microscopy, or a spherical crystal for microradiography) and give the soft-X-ray microscope and its microradiography images in a projection mode. With both techniques using projection, it is possible to produce a magnification $M > 1$, regulated by the distance of the sample and the photosensitive material from the optical element. (Flora et al., 2001).

Microradiography, at an energy of ~1 keV, was utilized for imaging internal structures of small insects like a mosquito (Albertano et al., 1997b; Bollanti et al., 1998; Flora et al., 2001; Pikuz et al., 2001). With this technique, a resolution of ~1 μm was obtained, because of the small size of the laser-plasma X-ray sources (small penumbra blurring). In this case, the photosensitive plate is typically a thin grain photographic film such as Kodak-RAR.

Generally, for microradiography of leaves, the 1-keV radiation represents the best compromise between the need for transparency of the leaf structure and X-ray absorption delineating the leaf details, producing a high contrast image.

In principle, many different targets can be used as the laser plasma X-ray source for imaging biological samples, since any heavy metal element used as a target in a laser plasma emits X-rays at wavelength values which are strongly absorbed by the same element. To look at structures inside leaves, where a specific heavy metal is supposed to be present, it is convenient to use a source with the same metal as the target. Therefore, among the imaging and analytical technologies, the X-ray microradiography and SXCM is very useful, since it allows the presence of almost any element to be localized.

The contrast within the leaf image can be increased by increasing the intake of different metals or by treating leaves with a heavy metal solution for some hours or days before being imaged.

The principal aim of this study is to demonstrate the detection, using X-ray imaging of the leaves, the uptake storage sites of chemical elements (e.g., heavy metal pollutants). In particular, a copper sulfate solution has been used to dope leaves which have then been exposed to X-ray radiation produced from a Cu target in order to visualize where Cu was mainly located.

MATERIALS AND METHODS

Characteristics of the X-ray Source

A high-power Nd:glass laser has been used with various metal targets for producing an X-ray source suitable for soft-X-ray contact microradiography of plant leaves (Bellucci et al., 2000; Petrocelli et al., 1993a,b). This laser has a pulse energy around 8 J and a pulse duration of 15 ns. The laser beam is focused on a target of copper material placed in the middle of a vacuum chamber (Bellucci et al., 2000; Petrocelli et al., 1993a,b).

A scheme of the experimental layout for contact microradiography mentioned above is shown in Figure 2.

The X-ray source diameter is rather large ($\oslash \sim 300$ μm) due to the low numerical aperture (NA ~ 0.03 μm) of the focusing lens. The distance from the plasma source and the sample holder is $d = 15$ cm.

The relatively large size of the source could give some problems of penumbral blurring. For this reason, the sample is placed as close as possible to the film (at ~1 mm). In this case, the expected penumbra blurring is just 2 μm, comparable with the grain size of the RAR film emulsion used in the film plate. The visible light was filtered by a 2-μm thick polypropylene foil coated with a 0.4-μm thick aluminum layer, with a total thickness of 2.4 μm.

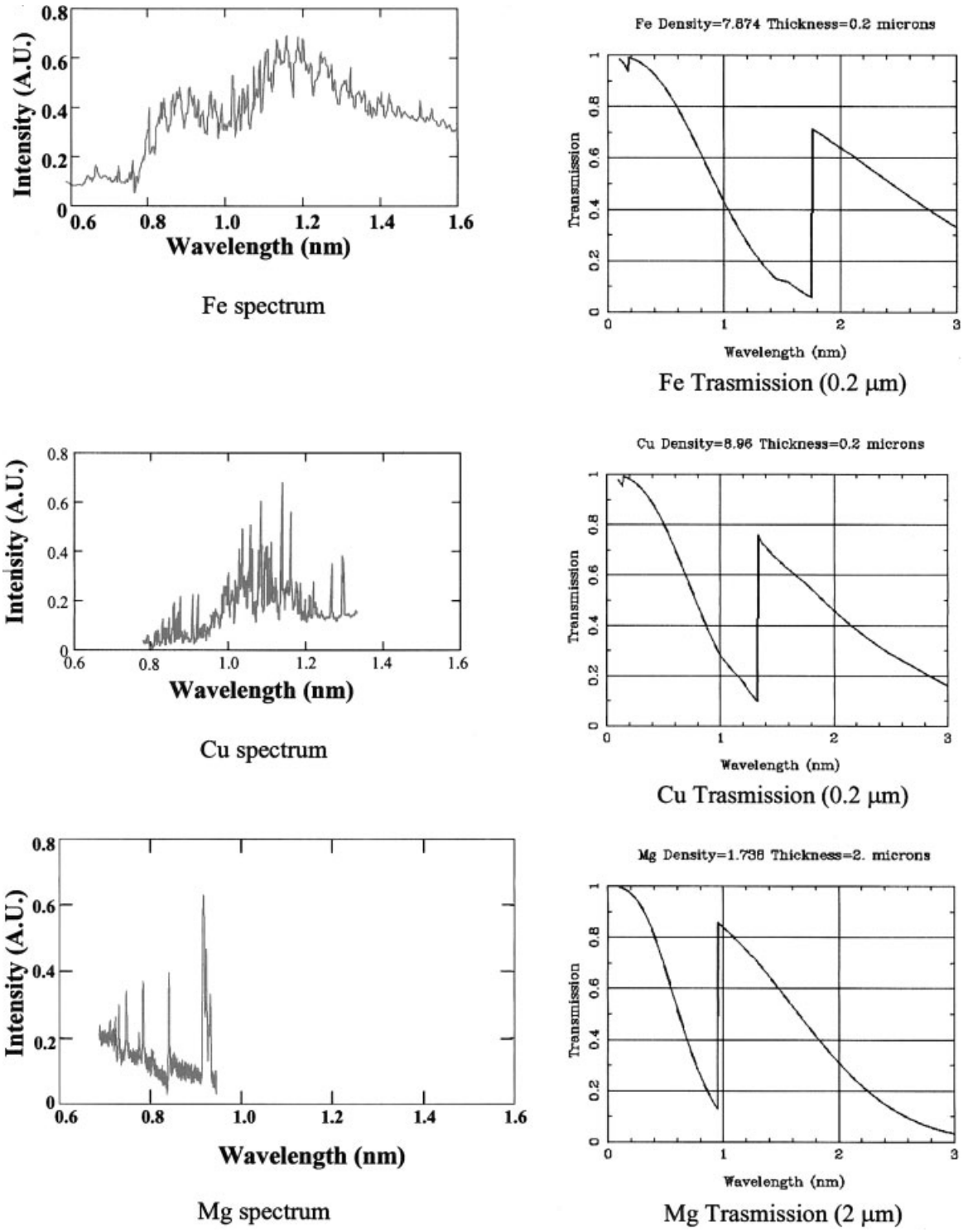

Fig. 3. Emission spectra of Fe and Cu targets (mainly by Ne-like ions) and of a Mg target (mainly by the He-like ions) in a plasma heated by a laser pulse having an intensity of 10^{13}–10^{14} W/cm^2 (left side) and corresponding absorption spectra (right side).

The laser equipment was designed and manufactured by Quantel, located at Rome University "Tor Vergata," STFE (Scienze e Tecnologie Fisiche ed Energetiche) Department, INFM (Italian National Institute for Physics of Matter) Tor Vergata Research Unit.

Figure 3 compares the emission and transmission spectra of three different strong emitter materials in

the 1-keV region. These data are taken from the literature for laser plasmas at intensities similar to those utilized in this article. In particular, Fe and Cu emission spectra are extracted from Boiko et al.(1985); the Mg spectrum is obtained from a laser plasma source pumped by a Nd laser (Bellucci et al., 2000), while the absorption spectra are given by Henke et al. (1993).

From this picture, the expected correspondence of the strongest emission by Ne-like Cu or Fe ions (that is, ions depleted of electrons up to remaining with the same number of electrons as the neutral neon atom, that is, 10 electrons) and by He-like Mg ions (that is, Mg ions with just 2 electrons, as helium) with the strongest absorption spectra occurring for copper or iron or magnesium is clear.

In fact, the spectral regions of highest emission for iron, copper, and magnesium lay on the left side of the corresponding absorption L-edge wavelength at 1.753 and 1.330 nm for iron and copper, and of the absorption K-edge wavelength at 0.951 nm for magnesium. In these emission ranges lies the poorest transmission for each of the three metals: that is, only 20% for the thickness of 0.2 μm for Fe and Cu and thickness of 2 μm for Mg, both thickness values being chosen as examples in the figure. Practically, no lines are emitted, for each element, at wavelengths lying on the right side of the corresponding absorption edge; these regions of the emission spectra are not reported in the figure.

A thickness of magnesium 10 times larger than that of Fe and Cu is necessary to reach the equivalent transmission value (20%) at the absorption edge. This higher thickness requirement could theoretically limit the possibility to detect the areas of biological samples which are rich in magnesium, unless the magnesium amount itself is very large. For this reason, the presence of Mg has not been pursued in these first experiments.

Between Cu and Fe, Cu has been selected because copper sulfate solution can be used to dope leaves as a possible contaminant/pollutant. Copper compounds are also tolerated by the plant as compared with iron salts; in fact, iron is found naturally in soils and is not a pollutant.

One-month-old *Viola x wittrockiens* (dicotyledon, angiosperm) plants, grown in flasks containing 1:1:1 clay:sand:peat, were used in this experiment, and only one (i.e., copper) of the three elements mentioned earlier was used for doping treatment of the plants.

Different solutions of copper sulfate ($CuSO_4$) were employed for uptake into the leaves. In fact, the leaves of the plant *Viola x wittrockiens* were treated for a time of 24 h with three different concentrations of copper sulfate: (a) 1%, (b) 2%, and (c) 5%. Untreated leaves were used as control.

Before being imaged, all the leaves were dried with increasing concentrations of alcohol (50, 70, 80, 95% and absolute) to eliminate any residual water, which might strongly absorb X-rays. Furthermore, the use of predehydrated leaves avoided any alteration of their structure during the experiment in the vacuum chamber.

Leaves were fixed in a dark chamber in contact with the photographic film RAR 2492. In all cases, only one shot of the Nd:laser beam was sufficient to obtain a good exposure of this photographic film placed at 15 cm from the target. The corresponding measured fluence on the samples is about 130 $\mu J/cm^2$. The exposure time was 15 ns. This very short exposure time avoided any movement blurring in the images.

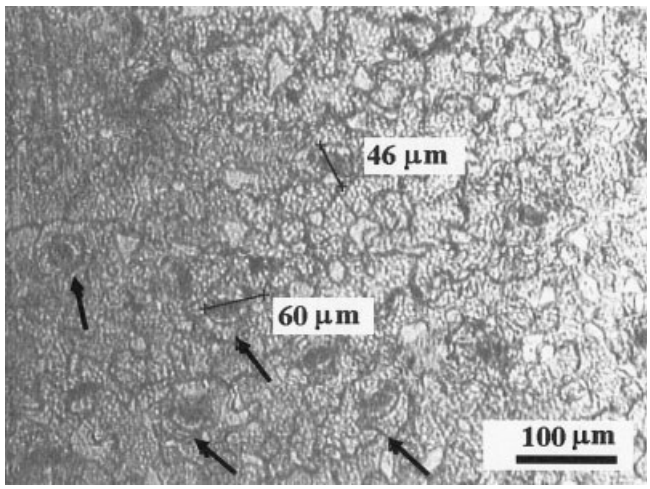

Fig. 4. Lower external epidermis layer of leaf of *Viola x wittrockiens* (at optical microscope) showing size of cells and diameter of stomata (arrows indicate stomata; the black lines sign up their diameter); (objective lens 10×).

After the exposure to X-rays, the films were developed in Ormano Bromor ST-50 diluted 1:4 and fixed in Ormano Superfix F205 diluted 1:4, for 5 min each. The images obtained were digitized with a scanner.

We have imaged four kinds of dried leaves by contact microradiography: control leaves (a) and three different kinds of leaves ((b)–(d)) treated with the three concentration levels of copper sulfate solution mentioned above.

RESULTS AND DISCUSSION

Genus *Viola x wittrockiens* was chosen for its easy availability. It should be also pointed out that a related species, *Viola calaminaria*, has been extensively studied for phytoremediation and shown to bioaccumulate up to 1% zinc in dry leaves (Salt et al., 1998); moreover, the same *Viola calaminaria* has also been studied for association with michorrizal fungi, which improved its phytoremediation properties (Hildebrandt et al., 1999; Kaldorf et al., 1999).

Before exposing leaves of *Viola x wittrockiens* to X-rays, they were directly analyzed under an optical microscope for comparison with the subsequent radiographs.

Optical microscope images of the lower epidermis are shown in Figure 4; the stomata and their dimensions are also indicated.

Soft-X-ray microradiographs obtained with the Cu target of the control (a) and of the treated leaves corresponding to the two different doping values, 1% (b) and 5% (c), are shown in Figure 5.

Different structures are visible in form of spherical granules (the white dots corresponding to X-ray opaque zones). These granules are more evident for the higher doping concentrations and they appear to have different size and shape. Furthermore, a content of copper could be hypothesized for them; the main and secondary veins are also more X-ray absorbent in the doped leaves. The average dimension of grains is around 50 μm.

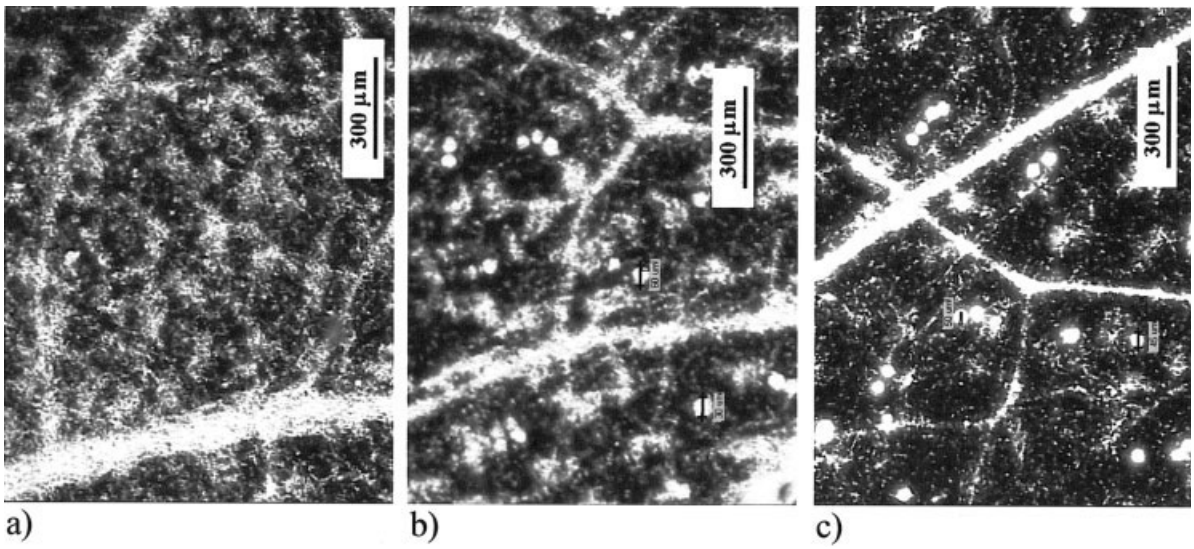

Fig. 5. Details of the X-ray images on the photographic film RAR 2492 observed under a 40× objective lens optical microscope: (**a**) control detail, (**b**) 1% treated detail, and (**c**) 5% treated detail. Average dimension of grains is ~50 µm in diameter.

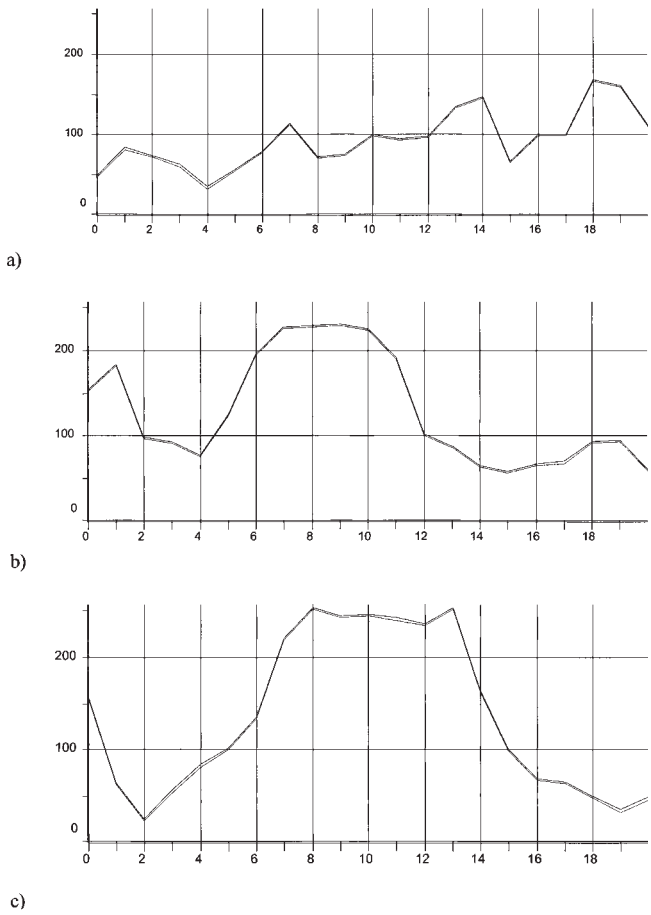

Fig. 6. Grayscale levels at 8-bit on the grains in the three doping images: (**a**) control, (**b**) 1% treatment, and (**c**) 5% treatment.

In Figure 5, in fact, it is possible to note that there are few large granules in the control leaf images, while the granules appear very clearly in the treated leaves and show a stronger contrast for increasing salt concentrations.

This is shown more clearly in Figure 6, where the grayscale levels, directly measured on the grain area in the three different microradiographs, are reported. As it can be seen in this figure, at the highest doping level (5%), grains reach the highest gray level contrast value and the biggest size; for the middle treatment (1%), the grain contrast is a bit lower, while the control detail seems to be without any relevant contrast peaks.

The microradiographs can be evaluated quantitatively by measuring their optical density (OD). To obtain these data, it is necessary to measure the grayscale level in the image and then evaluate the OD by using the scanner's calibration curve obtained by scanning calibrated neutral optical filters, and using the same scanner at a fixed optical gain.

In Figure 7, the profiles of the OD obtained on the microradiographs by averaging the OD (x, y) along the vertical coordinate (y) are shown. Also included in the graph are the average values for each treatment (that is, the O.D. value averaged on the whole area), shown better in Figure 8. The variation of OD due to the doping, hidden by the large local fluctuations, is well highlighted by this average OD on the whole image.

The apparent anomalous shift of the behavior of OD versus the doping level (see Fig. 8) is due to the fact that the control leaf and 1% doped leaf sample are imaged on one radiograph (with one laser shot), while the 2% and 5% doped leaf samples are imaged on another radiograph (with a higher laser shot energy). This shift disappears by normalizing the OD values to the laser shot energy.

This is indirectly shown in Figure 9, where the average transmission of all samples is reported.

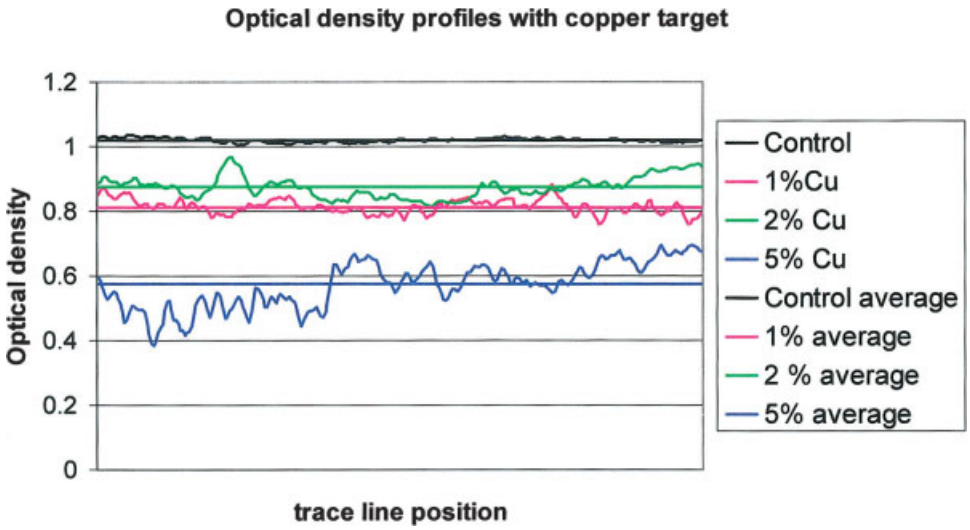

Fig. 7. Profiles of the OD of the microradiographs obtained by averaging the OD (x, y) along the vertical coordinate (y). The graph also includes the average values for each treatment.

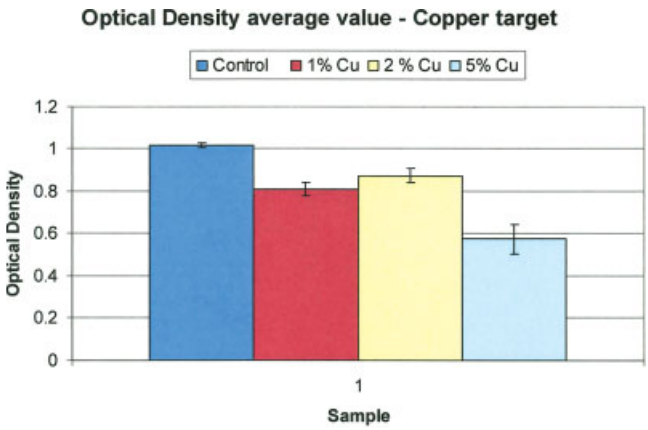

Fig. 8. OD average values on the microradiographs of the different samples (bars represent ±SD).

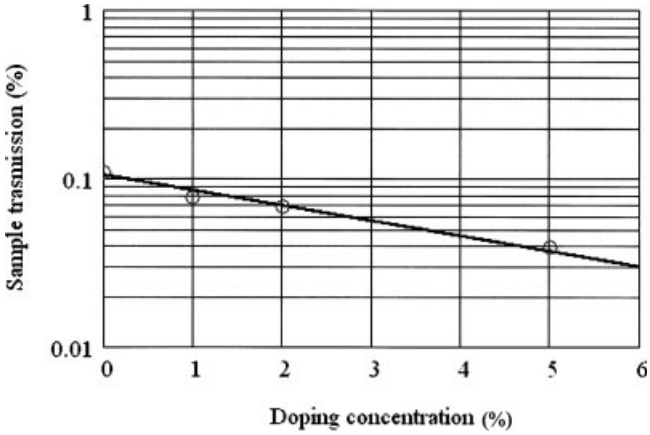

Fig. 9. Leaf transmission for the different doping values.

In fact, starting from the average values of the OD and considering the response of the RAR 2492 film (ref. Henke et al., 1993 II experimental characterization), it is possible to convert the OD values of Figure 8 into fluence values, that is:

$$F = (e^{\text{O.D.}/A} - 1)/S \quad (1)$$

where for a photon energy between 0.9 and 1.5 keV, it is $A = 1.1$ and $S = 12$ cm^2/μJ.

From the values of fluencies and from the value of fluence in the direct film exposure region (that is, the regions not shadowed by samples), it is possible to obtain the leaf transmission values for the different doping values by:

$$T_i = F_i/F_{\text{direct}} \quad (2)$$

where i pinpoints at all the doping values including the control.

As it can be seen in Figure 9, these average transmission values of our samples in the 1-keV region are much less than 1%; but exactly for this reason, the sensitivity to doping is high. For higher photon energies, the transmission of samples would be much higher, but the sensitivity to the doping would be lost.

It is interesting to note how the averaged transmission decreases as the concentration of the copper sulfate solution treatments increases.

Then, considering that all the leaves were grown in similar conditions and have the same thickness, the increment of absorption of the doped leaves can be attributed just to the copper absorbed by the leaves. It is also possible to measure the transmission due only to the copper intake, by dividing the total transmission of each doped samples by the transmission of the control leaf:

$$T_{\text{Cu}\,i} = T_i/T_{\text{control}} \quad (3)$$

Finally, from the Cu transmission, it is possible to estimate the Cu surface density (ρh, that is the density ρ integrated over the leaf thickness h) in the different

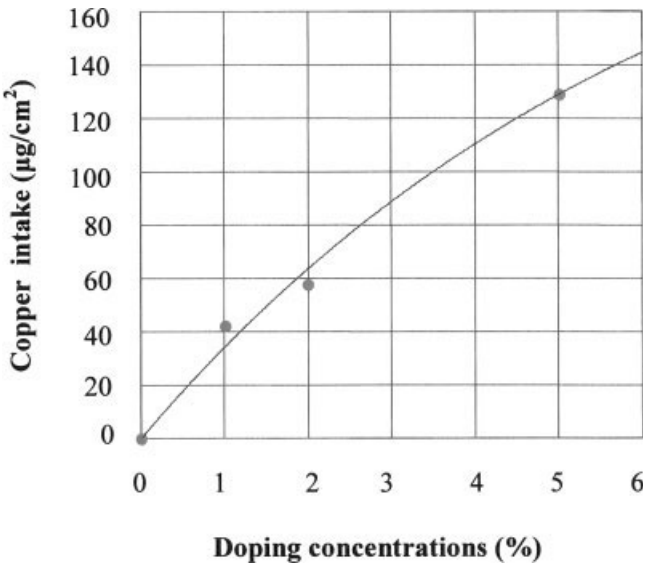

Fig. 10. Copper intake in the doped leaf samples versus the treatment concentration. The copper intake is estimated from the average OD of the related radiographs.

TABLE 1. Cu intake values according with concentration in $CuSO_4$ in the doping solution

Cu concentration in the doping solution (%)	0	1	2	5
Cu intake by the leaves (μg/cm²)	0	42.00	57.76	128.87

doped leaves by:

$$\rho h = \frac{\ln\left(1/T_{\mathrm{Cu}\,i}\right)}{\mu_{\mathrm{M}}} \tag{4}$$

where μ_M is the mass absorption coefficient of copper ($\sim$8,000 cm^2/g at an energy value of 1.2 keV).

These values of copper density are shown in Fig. 10 and also in Table 1. In Figure 10, the experimental values of the copper intake are well fitted by the exponential behavior:

$$\mathrm{Cu}_{\mathrm{intake}} = A\left(1 - e^{-\mathrm{doping}/B}\right) \tag{5}$$

where the asymptotic value is $A = 0.24$ mg/cm^2 and the saturation doping treatment is $B = 6.5\%$.

From Figure 10, it is interesting to note that for the maximum doping level tested in our experiments (that is, 5% $CuSO_4$ in water), a Cu intake as high as $\rho h =$ 130 μg/cm^2 is reached, which is equivalent to a solid copper foil thickness $h = \rho h/\rho = 145$ nm. This equivalent Cu thickness gives at 1.2 keV an absorption of more than 60%, as seen in Figure 9, which is easily detectable. But the same copper thickness at the copper absorption K-edge of $\sim$9 keV would give an absorption of only 1% and 4% on the left and right side of the edge, respectively. This small transmission difference (usually applied in the dual energy technique) would be still detectable, but only if a CCD camera with a good linearity and stable response is used, such as, for example, the modern cooled 16-bit CCD camera.

From the microradiography observation under optical microscope (40×), the presence of granules is clear (see Fig. 5) and the granules are more visible in the treated samples than in the control ones.

Two main hypotheses for the particular nature of such granules are proposed.

First, they could be granules due to crystal contained in the copper sulfate treatment solution, which present into intercellular spaces among the cell, and the apoplast (Kosegarten and Koyro, 2001). This is in agreement with the observation on water and ion supply by xylem elements within the main and minor veins (Hans-Walters, 1999; Siebke and Weis, 1995; Taiz and Zeiger, 1996).

Second, it is also possible that these granules represent the vacuoles of some cells. In fact, copper ions from the apoplast could enter the cell membranes, and from the cytosol they could reach the larger structure inside the cell, the vacuole, where probably copper sulfate solution may especially accumulate. The vacuole almost occupies the whole volume of the cell and is a place where intake of contaminants is especially high. (Salt et al., 1998) In this way, it is possible that some cells bioaccumulate the contaminant solution in the vacuole; in fact, in the microradiography, the circular shape of possible vacuoles is clearly visible. This is a quite similar effect that takes place with the formation of druses of calcium oxalate that especially grow inside the vacuole in the cell.

It should be pointed out that no actual morphological analysis of the image details of the leaf was done, but was only hypothesized how to find a right way to highlight the intake of contaminant in the leaf. This means that, at the moment, it is important to show the possibility to detect the intake of contaminants, i.e., copper, in the leaf tissue, rather than recognizing a definite structure in the morphology of the cell.

Further studies could clarify the exact nature of these granules, which are observed here for the first time by microradiography (there is no previous result to compare).

The possibility that granules are artifacts due to the drying process can be excluded because they are present either if the leaves have been dried by hot air or by an increasing concentration of alcohol (as it has been done in the experiments of Fig. 5).

Grains are just visible in the control samples not treated with copper, indicating they are a normal structure of the leaf. Therefore, it appears that copper sulfate solution within the leaves just increases the absorption signal of the granules.

CONCLUSIONS

Contact microradiography images of leaves of *Viola x wittrockiens* have been obtained by using the $\sim$1-keV soft X-rays emitted by a laser-plasma source; the capabilities of this investigation as a method for the leaf metal-intake measurement have been analyzed by growing plants in the presence of different copper sulfate concentrations.

The amount of copper intake inside the leaf structures has been quantitatively determined starting from the analyses of the OD of the microradiographs. A graph of the detected amounts shows an almost linear relationship between the concentration of copper in

the doping solution and the intake in the leaf structures.

The inner structure of the leaf, with main and minor veins, has been imaged together with some round granules. As a first attempt to recognize the nature of these granules, two different hypotheses have been provided: they could be granules due to crystal of the copper sulfate treatment solution, or vacuoles within cells. Further studies should clarify their exact nature.

It is important to note that this X-ray technique images leaves differently when compared with the imaging of other methods. The two epidermis layers in the upper and bottom sides of the leaf nor the mesophyll cells between them cannot be distinguished from each other with this technique. One sees the leaf because of cumulative absorption results from many layers one above the other in the leaf tissues.

That the granules are drying artifacts seems to be excluded. The granules are always present (either by heat or alcohol drying), and their presence in the control leaves means that they are structures already present before treatment, while the $CuSO_4$ treatment only increases the contrast in the X-ray images.

Contact microradiography is a straightforward application of laser-plasma sources to biology (Reale et al., 2004). In the experiments presented here, the use of a wide spectral distribution of the X-rays has significantly limited the sensitivity on recognizing the chemical nature in the different leaves' structures. The imaging with monochromatic X-ray radiation obtained through a reflection on a spherically bent crystal (Pikuz et al., 2001) is scheduled for future studies.

The use of monochromatic radiation, and hence the possibility to apply the dual-imaging-subtraction technique, will improve the capability of applying this method in phytoremediation studies. (Kamnev and van der Lelie, 2000; Khan et al., 2000; Meagher, 2000). Moreover, it could provide information on the health status of a plant.

A dual energy analysis is the subtraction between two images of the same sample obtained at two slightly different wavelengths opposite each other, with respect to the absorption edge of a specific chemical element. This technique will allow not only the chemical mapping of the sample, but also increasing the sensitivity to the chemical abundance by an order of magnitude or more, so that the amount of such chemicals can be estimated in treated and nontreated leaves. Of course, the CCD detector will need to have a high dynamic range like the modern cooled 16-bit CCD.

If a plant is grown in a heavy metal polluted environment and has adsorbed elemental pollutants from the ground, this X-ray technique could in principle show the presence of such elemental pollutants in the plant tissues.

It could be very important to detect the intake of heavy metals into a plant in the early stage of the process; for this purpose, X-ray microradiography of leaves or other plant tissues could be a very useful tool.

It is evident that further experiments are needed to better characterize microradiography of biological samples as a tool for their heavy metal chemical mapping, although it should be clear that this technique can provide useful results.

ACKNOWLEDGMENTS

The authors thank Dr. Anna Ragnelli and Dr. Loretta Pace of the Biology Department of University of L'Aquila for interesting suggestions during the analyses of images.

The authors thank also Dr. Anna Scafati for support during the set up of the experiment and writing of the article.

The authors also thank Consorzio di Ricerca Gran Sasso for the support given.

REFERENCES

Albertano P, Reale L, Palladino L, Reale A, Cotton R, Bollanti S, Di Lazzaro P, Flora F, Lisi N, Nottola A, Vigli-Papadaki K, Letardi T, Batani D, Conti A, Moret M, Grilli A. 1997a. X-ray contact microscopy using an excimer laser plasma source with different target materials and laser pulse durations. J Microsc 187:96–103.

Albertano P, Belli M, Di Lazzaro P, Faenov AYa, Flora F, Grilli A, Letardi T, Nottola A, Palladino L, Pikuz T, Reale A, Reale L, Scafati A, Tabocchini A, Turcu EIC, Vigli-Papadaki K. 1997b. Atmospheric pressure soft-X-ray source, for contact microscopy and radiobiology applications. SPIE Int Conf Opt Sci 3157:164–175.

Bellucci I, Ciuffa P, Flora F, Martellucci S, Petrocelli G. 2000. Spettroscopia ad alta risoluzione di un plasma di Mg. Collana di quaderni di ottica e fotonica N. 7– Societa' italiana di ottica e fotonica. 40 Anni di laser – Firenze 28-11-2000:159–162.

Boiko VA, Vinogradov AV, Pikuz SA, Skobelev IYu, Faenov AYa. 1985. The X-ray spectroscopy of laser produced plasma. J Sov Laser Res 6:85–290.

Bollanti S, Di Lazzaro P, Letardi T, Schina G, Zheng CE, Filippi L, Palladino L, Reale A, Taglieri G, Batani D, Mauri A, Belli M, Scafati A, Reale L, Albertano P, Grilli A, Faenov AYa, Pikuz T, Cotton AR. 1995. Long-duration soft X-ray pulses by XeCl laser driven plasmas and applications. J X-ray Sci Technol 5:261–277.

Bollanti S, Cotton R, Di Lazzaro P, Flora F, Letardi T, Lisi N, Batani D, Conti A, Mauri A, Palladino L, Reale A, Belli M, Ianzini F, Scafati A, Reale L, Tabocchini MA, Albertano P, Faenov AYa, Pikuz T, Oesterheld A. 1996. Development and characterisation of an XeCl excimer laser-generated soft-X-ray plasma source and its applications. Nuovo Cimento D 18:1241–1255.

Bollanti S, Albertano P, Belli M, Di Lazzaro P, Faenov AYa, Flora F, Giordano G, Grilli A, Ianzini F, Kukhlevsky SV, Letardi T, Nottola A, Palladino L, Pikuz T, Reale A, Reale L, Scafati A, Tabocchini MA, Turcu ICE, Vigli-Papadaki K, Schina G. 1998. Soft X-ray plasma source for atmospheric-pressure microscopy, radiobiology and other applications. Nuovo Cimento D 20:1685–1702.

Conti A, Batani D, Botto C, Masini A, Bernardinello A, Bortolotto F, Moret M, Poletti G, Piccoli S, Cotelli F, Lora Lamia Donin C, Stead A, Marranca A, Eidman K, Flora F, Palladino L, Reale L. 1997. Contact X-ray microscopy using Asterix. SPIE Proc 3157:218–230.

Cotton RA. 1992. Soft x-ray contact microscopy: a new technique for the life sciences. Microscopy and Analyses September 15–17.

Cotton R, Bollanti S, Di Lazzaro P, Flora F, Lisi N, Letardi T, Palladino L, Reale A, Batani D, Conti A, Mauri A, Moret M, Reale L, Albertano P, Grilli A. 1995. X-ray contact microscopy using a plasma source generated by long and short (120 ns and 10 ns) excimer laser pulses. SPIE Proc 2523:184–193.

RA, Dooley MD, Fletcher JH, Stead AD, Ford TW. 1992. Atomic force microscopy employed as the final imaging stage for soft X-ray contact microscopy. SPIE Proc 1741:204–212.

Fletcher JH, Cotton RA, Webb CE. 1992. Soft X-ray contact microscopy using laser generated plasma sources. SPIE Proc 1741: 142–153.

Flora F, Bollanti S, Lai A, Di Lazzaro P, Letardi T, Grilli A, Palladino L, Tomassetti G, Reale A, Reale L, Scafati A, Bacchetta L, Alainelli L, Sanchez Del Rio M, Pikuz T, Faenov AYa. 2001. A novel portable, high-luminosity monochromatically tuneable X-ray microscope. Application of X-rays generated from lasers and other bright sources II. Proc SPIE 4504:240–252.

Ford TW, Stead AD, Cotton AR. 1991. Soft-x-ray contact microscopy of biological specimens. Electron Microsc Rev 4:269–292.

Hans-Walters H. 1999. Plant biochemistry and molecular biology. Oxford: Oxford University Press.

Henke BL, Gullikson EM, Davis JC. 1993. X-ray interactions: Photoabsorption, scattering, transmission and reflection at E = 50–30000 eV, Z = 1–92. Atomic Data Nucl Data Tables 54:181–343.

Hildebrandt U, Kaldorf M, Bothe H. 1999. The zinc violet and its colonization by arbuscular mycorrhizal fungi. J Plant Physiol 154:709–717.
Kaldorf M, Kuhn AJ, Schroder WH, Hildebrandt U, Bothe H. 1999. Selective element deposits in maize colonized by a heavy metal tolerance conferring arbuscular mycorrhizal fungus. J Plant Physiol 154:718–728.
Kamnev AA, van der Lelie D. 2000. Chemical and biological parameters as tools to evaluate and improve heavy metal phytoremediation. Biosci Rep 20:239–258.
Khan AG, Kuek C, Chaudhry TM, Khoo CS, Hayes WJ. 2000. Role of plant, mycorrhizae and phytochelators in heavy metal contaminated land remediation. Chemosphere 41:197–207.
Kosegarten H, Koyro HW. 2001. Apoplastic accumulation of iron in the epidermis of maize (*Zea mays*) roots grown in calcareous soil. Physiol Plant 113:515–522.
Meagher R. 2000. Phytoremediation of toxic elemental and organic pollutants. Curr Opin Plant Biol 3:153–162.
Medenwaldt R, Abraham-Peskir J, Uggerhøj E. 1998. X-ray microscopy in Aarhus with 30 nm resolution. Synchrotron Radiat News 11:39–43.
Panessa BJ, McCorkle R, Hoffman P, Warren JB, Coleman G. 1981. Ultrastructure of hydrated proteoglycans using a pulsed plasma source. Ultramicroscopy 6:139–148.
Panessa-Warren BJ, Tortora GT, Warren JB. 1989. Absorption edge imaging of bacterial endospores with synchrotron radiation. Ultramicroscopy 27:151–160.
Panessa-Warren BJ, Tortora GT, Stears RL, Warren JB. 1991. Biological calcium adsorption edge imaging using monochromatic synchrotron radiation. Ultramicroscopy 36:277–296.
Petrocelli G, Martellucci S, Richetta M. 1993a. Bismuth induced enhancement of the second-harmonic generation efficiency in bismuth- substituted yttrium iron garnet film. Appl Phys Lett 63: 3402–3404.
Petrocelli G, Pichini E, Scudieri F, Martellucci S. 1993b. Anisotropic effects in the third-harmonic generation process in cubic crystals. J Opt Soc Am B 10:918–923.
Pikuz T, Faenov YaA, Fraenkel M, Zigler A, Flora F, Bollanti S, Di Lazzaro P, Letardi T, Grilli A, Palladino L, Tomassetti G, Reale A, Reale L, Scafati A, Limongi T, Bonfigli F, Alainelli L, Sanchez del Rio M. 2001. Shadow mono chromatic backlighting: Large-field high resolution X-ray shadowgraphy with improved spectral tunability. Laser Part Beams 19:285–293.
Reale L, Lai A, Tucci A, Poma A, Faenov A, Pikuz T, Flora F, Spanò L, Limongi T, Palladino L, Ritucci A, Tomassetti G, Petrocelli G, Francucci M, Martellucci S. 2004. Differences in X-ray absorption due to cadmium treatment in *Saponaria officinalis* leaves. Microsc Res Tech 64:21–29.
Salt DE, Smith RD, Raskin I. 1998. Phytoremediation. Annu Rev Plant Physiol Plant Mol Biol 49:643–648.
Siebke K, Weis E. 1995. Imaging of chlorophyll-a-fluorescence in leaves: Topography of photosynthetic oscillations in leaves of *Glechoma hederacae*. Photosynth Res 45:225–237.
Stead AD, Ford TW, Myering WJ, Clarke DT. 1988. A comparison of soft X-ray contact microscopy with light and electron microscopy for the study of algal cell ultrastructure. J Microsc 149:207–216.
Stead AD, Cotton RA, Page AM, Dooley M, Ford TW. 1992. Visualization of the effects of electron microscopy fixative on the structure of hydrated epidermal hairs of tomato (*Lycopersicum peruvianum*) as revealed by soft-X-ray contact microscopy. SPIE Proc 1741:351–362.
Taiz L, Zeiger E. 1996. Fisiologia vegetale. Padova: Piccin.